The role played by the polarization potential in the elastic scattering of light exotic nuclei on protons and carbon

V. LAPOUX *, N. ALAMANOS, F. AUGER, V. FÉKOU-YOUMBI,
A. GILLIBERT, F. MARIE, S. OTTINI-HUSTACHE, J. L. SIDA
CEA-SACLAY,DSM/DAPNIA/SPhN 91191 Gif-sur-Yvette Cedex, FRANCE
**E-mail: vlapoux@cea.fr*

D. T. KHOA
Vietnam Atomic Energy Commission, Hanoi

J-M. CASANDJIAN, M-D. CORTINA-GIL, M. CHARTIER, M. MAC CORMICK, W.MITTIG,F. de OLIVEIRA, P. ROUSSEL-CHOMAZ
GANIL, Bld Henri Becquerel, BP 5027, 14021 Caen Cedex, France

N. ORR, J.WINFIELD
LPC-ISMRA Bld du Maréchal Juin, 14050 Caen Cedex, France

Y. BLUMENFELD,J. KELLEY, F. MARÉCHAL, J-A. SCARPACI, T. SUOMIJÄRVI
IPN 15 rue Georges Clémenceau, Bât 100 91406 Orsay CEDEX

Elastic scattering is sensitive to the interaction potential between target and projectile and to the microscopic structure of the nuclei involved, and light exotic nuclei are a laboratory to investigate nuclear matter far from the stability valley. So we have measured differential cross sections of elastic scattering reactions involving radioactive beams of light exotic nuclei (^{6}He, ^{10,11}Be) on targets of ^{12}C and protons. Thanks to the good energy resolution of the energy-loss spectrometer SPEG at GANIL, these data do not include contaminations by scattering on the excited states of the target. Therefore, it is possible to investigate the effect of the weak binding of exotic nuclei on the elastic scattering data and to test the validity of the effective nucleon-nucleon NN interactions. The treatment of the polarisation potential is explained.

1 Motivations

Exotic nuclei are weakly bound, and so they can easily decay to cluster states. One dramatic consequence is the neutron halo structure that light neutron-rich nuclei such as ^{11}Li can exhibit : ^{11}Li can be described as a core with one or two neutrons with a high probability of being far apart from the core.

Another important effect of the weak binding is that the particle threshold for these nuclei is close to their ground state, which favours couplings to the continuum during their interaction with a target. For these nuclei one must

take into account the interaction potential term due to transitions going to the excited states and then back to the ground state. But its precise calculation requires the knowledge of the spectroscopy of the nucleus and also the knowledge of low-lying resonant states and couplings to the continuum. This term is called "polarization potential". It includes the break-up effects. Our aim in the analysis of cross sections of elastic scattering is to know whether the weak binding of exotic nuclei should appreciably enhance the polarization potential and to determine a general form of this potential. Thus, to study the effect of the weak binding on the potential of interaction between a light exotic nucleus and a target, we have measured angular distributions of cross sections of elastic scattering involving radioactive beams of light neutron-rich nuclei (^{10,11}Be and ^{6}He) on ^{12}C and protons at low energy (38.3 A.MeV).

2 Experimental device

Data were taken at GANIL (Caen, France). The SISSI (Superconducting Intense Source for Secondary Ions) and the SPEG (Energy Loss Spectrometer at GANIL) devices were used to produce the secondary beams and to detect the scattered particles, respectively. Elastic angular cross sections of ^{10,11}Be, and ^{6}He on targets of protons, ^{12}C were measured with the high resolution spectrometer SPEG. Secondary beams were produced by fragmentation of a 75 A.MeV primary ^{18}O beam, delivered by the two GANIL cyclotrons on a carbon production target located between the two superconducting solenoids of SISSI. ^{10}Be and ^{11}Be had an intensity of 10^5 pps and 3.10^4 pps, respectively, and an energy of 39.14 A.MeV and 38.43 A.MeV. ^{6}He was produced at 38.3 A.MeV and 10^5 pps during another experiment, with a ^{13}C primary beam of 75 A.MeV. The scattered particles were identified in the focal plane of SPEG by the energy loss measured in an ionisation chamber and the residual energy measured in plastic scintillators. The momentum and the angle after the target were obtained by track reconstruction of the trajectory as determined by two drift chambers located near the focal plane of the spectrometer. The energy resolution $\frac{\Delta E}{E} = 10^{-3}$ allows the measurement of elastic scattering angular distributions of light nuclei without the contaminations from target excitations. The angular resolution is of the order of 0.5^o in the laboratory sytem.

3 Nucleon-nucleus potential

The nucleus-nucleon elastic scattering can be described with a complex nucleon-nucleon interaction JLM [1] deduced from calculations with Brueckner matrix, performed in infinite symmetric nuclear matter with the local density approximation, and for energies up to 160 MeV. This model generates a complex

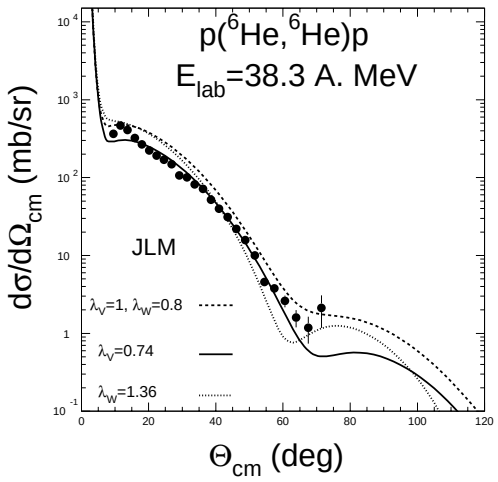

Figure 1: Angular cross sections of ^{6}He + p elastic scattering at 38,3 A.MeV. Curves are calculated with the JLM potential. Full line (respectively dotted line) corresponds to calculations in which the real part (imaginary) was renormalized. The dashed line corresponds to the usual factor for light nuclei in the JLM potential : λ_V=1, λ_W = 0,8.

microscopic potential which only depends on the scattering energy and on the density of the involved nucleus. In the case of stable nuclei, it reproduces successfully a large range of proton and neutron elastic scattering angular distributions, without any free parameter[2]. In the case of light exotic nuclei, data are well reproduced, provided the imaginary potential be somewhat adjusted by a normalization factor $\lambda_W \sim 0.8$.

3.1 ^{6}He + p elastic scattering

^{6}He+p is analyzed with the JLM potential, as shown in Fig 1. ^{6}He can be easily described by the three-body model[3] as a tightly bound alpha particle plus two valence neutrons, with the ^{6}He neutron separation energy (2n+α) of 0.975 MeV. The ^{6}He density included in the JLM calculation is a three-body density with a matter rms of 2,55 fm, close to the value obtained in the three-body model analysis[4] of the elastic scattering of ^{6}He on proton at intermediate energies[5]. The angular distributions of ^{6}He on proton are better reproduced when the real part of the JLM potential is scaled. This means that the break-up of the nucleus predominantly affects the real part. The origin of this effect can be explained with the Feshbach theory.

3.2 polarization potential

According to the Feshbach theory[6], the interaction potential should be written as : $U_E = V_{00} + \Delta U_{pol}$ with ΔU_{pol} the complex, non-local, energy-dependent, dynamical polarization potential (DPP), and V_{00} which includes only ground state ϕ_{P0} and ϕ_{C0} of the projectile and target particles : $U_F(\vec{R}) \equiv V_{00} = \langle \phi_{p0}\phi_{t0} \mid V \mid \phi_{p0}\phi_{t0} \rangle$. V_{00} is the usual potential which can be seen as the folding potential. The polarization potential comes from couplings to inelastic channels.
The more weakly bound the nucleus is, the greater the influence of ΔU_{pol}. This effect was studied in Ref. [7] for the elastic scattering of ^{11}Li on ^{12}C at 60 A.MeV. The normalization of the real part of the folding potential, needed when nuclei are weakly bound (^{11}Li) or can be considered as clusters (^{6}Li) accounts for the effect of the polarization potential, as seen in Ref[8]. It corresponds to the observed effect in the ^{6}He+p scattering, analyzed with the JLM potential (Fig 1). A complex surface potential, with a repulsive real part, is expected to simulate the surface effects generated by the polarization potential[8]. Like in Ref[9] we adopt a repulsive surface potential without radius :
$V_{pol} = -V_o \, \exp\left(\frac{r}{a}\right)/[1+\exp\left(\frac{r}{a}\right)]^2$ and $V_o \leq 0$. The nucleon-nucleus analysis with the JLM potential has shown that the break-up of the nucleus predominantly affects the real part, and the conclusions are similar with the CH89 optical potential parametrization[10] that we adopt for simplicity for the following analysis. V_{pol} is added to the optical potential and the result for the ^{6}He + p system is given in fig 2.

4 Nucleus-nucleus potential

4.1 Folding model

The real part of the potential of interaction between the exotic projectile and target is obtained by means of the folding model[11]. The imaginary one is taken from the optical model, usually it is a Woods-Saxon potential with three free parameters (W_I, a_I, r_I).

4.2 Effective NN interactions

A parametrization of the effective interaction was searched by the authors of Ref[12], which should satisfy the properties of saturation of the nuclear matter. They required, to simplify, that the parameters of the density-dependent part $\mathcal{F}$ of the interaction are independent of the energy. The energy dependence is in the factor $g(E)$, and the interaction is combined, as in the case of the

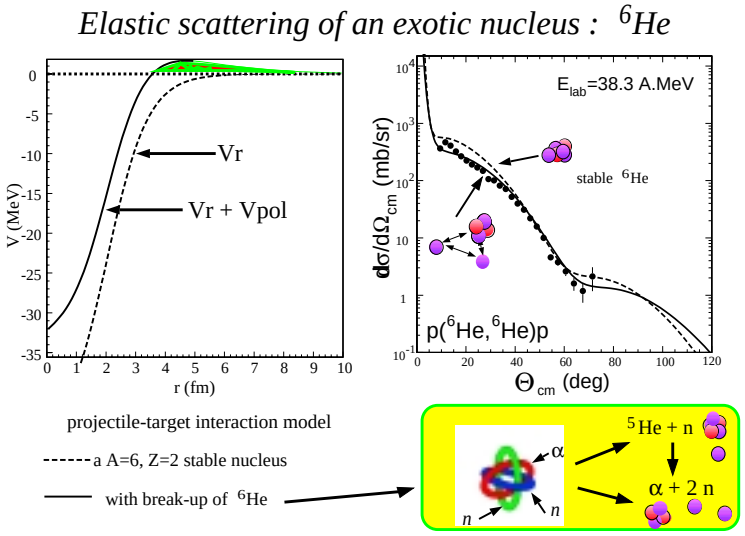

Figure 2: Angular cross sections of elastic scattering ^{6}He + p at 38.3 A.MeV. Data were measured at GANIL with the SPEG device. Lines are the results of calculations using the CH89 potential (dashed line) and taking into account a complex polarization potential added to CH89 (solid line). The real part of the DPP is represented on the left side of the figure. It is a surface potential simulating break-up effects whose parameters are $V_{pol} = -47,2$ MeV ; $a_{pol} = 1,33$ fm.

interaction DDM3Y[11], to the term $V^{M3Y}(r_{12})^a$ which can be the Reid or the Paris interaction with its exchange term treated explicitly, without making the assumption of the zero-range interaction. So the interaction is written :

$$V(r_{12},\rho,E) = V^{M3Y}(r_{12}) \times \mathcal{F}(\rho)g(E) = V^{M3Y}(r_{12}) \times \mathcal{F}(\rho)[1-\gamma(\frac{E}{A})]$$

A power-law density dependence was associated with the original Paris-M3Y interaction V^{M3Y} to create the interactions called CDM3Y6(Paris) :
$\mathcal{F}(\rho) = C[1+\alpha e^{-\beta\rho} - \gamma\rho]$. These new CDM3Y$n$ interactions were developed and applied successfully (see Ref[12]) to nucleus-nucleus systems for which the elastic scattering presents strong refractive patterns, as for instance, in the case of α + nucleus which is now examined in 4.3.

[a] 3 terms of Yukawa calculated from G-matrix.

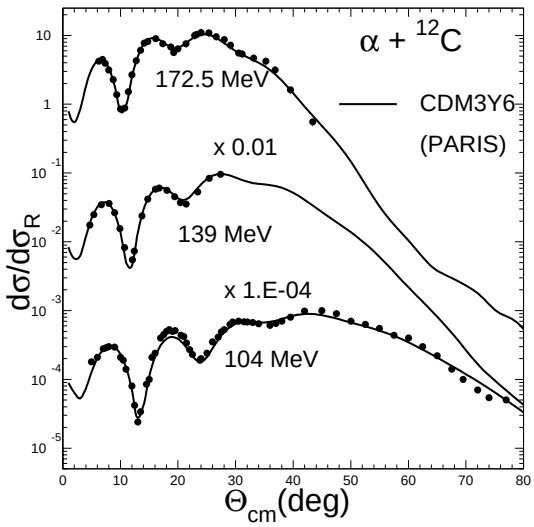

Figure 3: Elastic scattering data for $\alpha + {}^{12}$C, at 104, 139 MeV, and 172 MeV, are reproduced thanks to the real folding potential calculated with the CDM3Y6 interaction and thanks to the adjustment of imaginary part indicated in the text. Data references are given in the text.

4.3 Search for the core interaction with ^{12}C

The description by an interaction potential of the elastic scattering α+^{12}C is ambiguous. The folding model does not provide us with the imaginary part of the nucleus-nucleus potential. Moreover, it turns out to be necessary to normalize the real part by a factor N_r to reproduce elastic scattering data [13]. A larger set of data, in terms of incident energy, is needed in order to get rid of the uncertainties of the adjustment of N_r and of the imaginary part at one energy. The aim is to have a coherent variation of the N_r factor and of the parameters (W_i, a_i, r_i) of the imaginary part respected to the energy. So it will be possible to deduce the values at one energy of the range, in order to calculate the elastic scattering at that energy. We examine the $\alpha + {}^{12}$C data measured at the energy of $E_\alpha = 172.5$ MeV [14], at 139 MeV [15] and at 104 MeV [16]. We calculate the interaction potential $V_{\alpha+^{12}C}$ with the folding model which includes the effective NN interaction CDM3Y6 (Paris)[12], folded with the matter density of the α particle given in Ref. [11] and with the carbon one (2pF form, with rms equal to 2.2 fm). The imaginary part W is a Woods-Saxon

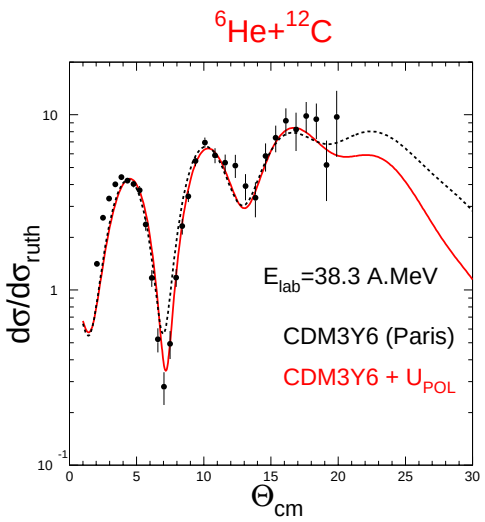

Figure 4: Elastic scattering data for ^{6}He + ^{12}C at 38,3 A.MeV are reproduced with a folded potential calculated with the CDM3Y6-Paris interaction and a gaussian-shape density for the ^{6}He. The dashed curve is realized with the CDM3Y6 potential. The solid curve is obtained by adding a complex surface potential which simulates the polarization potential : $V_{pol} = -64,4$ MeV ; $a_{pol} = 1,33$ fm.

potential, whose diffuseness a_I is fixed to 0,6 fm. The total potentiel can be written : $V_{\alpha+^{12}C} = N_r V_r + i\, W$. We adjust the depth W_I and the radius R_I of W, and the normalisation N_r, on the data. Data for the α + ^{12}C system at the different energies are well reproduced on Fig 3 by using $N_r = 1.3$ and the same imaginary part : W_I with a range from 18 to 21 MeV, $R_I = 3.75$ fm (reduced radius is r_i equal to 1.3 fm) and $a_I = 0.6$ fm.

4.4 ^{6}He-^{12}C elastic scattering

The real part of the potential of interaction between the exotic nucleus and ^{12}C is calculated in the framework of the folding model, including CDM3Y6. With an imaginary part W close to the one obtained in the description of α + ^{12}C elastic scattering ($W_I = 20$ MeV, $R_i = 4,64$ fm ($r_i = 1.13$ fm) and a_I =0,63 fm), and with a DPP deduced through the analysis of the scattering on protons the agreement with the data is satisfactory (see on Fig 4).

5 Conclusions

The potential of interaction between the exotic nucleus and ^{12}C was calculated in the framework of the folding model, including new density-dependent NN interactions like CDM3Y6. A complex surface potential, with a repulsive real part, is added to the optical potential. It can simulate the surface effects generated by the polarization potential. The obtained features for the polarization potential are in agreement with the theoretical predictions made by Y. Sakuragi [8].

We have shown that when the interaction which is involved in the folded potential is built in order to account for the saturation properties of the nuclear matter, and when it has the adequate density-dependences it can describe, together with a complex surface potential simulating the DPP, the elastic scattering of a weakly bound nucleus on a target. The weak binding of the exotic nuclei involves an increase of the break-up probabilities, and this effect must be taken into account in the study of reaction mechanisms at low energy.

Acknowledgments

We thank Dr I. J. Thompson for providing the ^{6}He density distributions in a tabulated form.

References

1. J.P. Jeukenne, A.Lejeune and C.Mahaux, *Phys. Rev.* C **16**, 80 (1977).
2. J.S.Petler & al, *Phys. Rev.* C **32**, 673 (1985).
3. B.V. Danilin & al., *Phys. Lett.* B **302**, 129 (1993).
4. J. Al-Khalili & al., *Phys. Rev.* C **54**, 1843 (1996).
5. G. D. Alkhazov & al, *Phys. Rev. Lett.* **78**, 2313 (1997).
6. H. Feshbach, *Theoretical Nuclear Physics (Wiley, New York 1992)*
7. D. T. Khoa, W. von Oertzen & al., *Phys. Lett.* **B 358** (1995) 14-20.
8. Y. Sakuragi, *Phys. Rev.* C **35**, 2161 (1987).
9. M. Hussein and G. Satchler, NP **A 567** (94) 165.
10. R.L. Varner & al., *Phys. Rep.* **201**, 57 (1991).
11. G.R. Satchler, W.G. Love ,*Phys. Rep.* **55**, 183 (1979).
12. D. Khoa, G. Satchler, W. von Oertzen, *Phys. Rev.* C **56**, 954 (1997).
13. M.E.Brandan and G.R. Satchler, *Phys. Rep.* **285** (1997) 143-243.
14. J. Kiss & al., *J Phys G* **13**, 1067 (1987).
15. S.M. Smith & al., *Nucl. Phys.* A **207**, 273 (1973).
16. Hauser & al *Nucl. Phys.* A **128**, 81 (1969).